

Turbulent Free Convection Enhancement in Square Cavities Driven by Different Gas Mixtures

Antonio Campo* and El Hassan Ridouane†
University of Vermont, Burlington, Vermont 05405
and

Mohammed M. Papari‡
Shiraz University of Technology, 71555-313 Shiraz, Iran

DOI: 10.2514/1.19470

The present paper investigates a promising avenue for the intensification of turbulent free convection in square cavities using an adequate selection of binary gas mixtures. Five binary gas mixtures have considered helium (He) as the primary gas component and carbon dioxide (CO₂), methane (CH₄), nitrogen (N₂), oxygen (O₂), and xenon (Xe) the secondary gas components. In the thermodynamic context, the thermophysical properties viscosity, thermal conductivity, density, and isobaric heat capacity depend on three quantities: temperature, pressure, and molar gas composition. The finite volume method is the vehicle used to perform the numerical calculations of the enlarged set of conservation equations, wherein turbulence is modeled with a low-Reynolds $k-\epsilon$ model. The turbulent velocity and temperature fields for each binary gas mixture and air were calculated at different locations in the cavity and presented in terms of streamlines and isotherms for $Ra = 2 \times 10^9$. The results culminate with the allied convective coefficient h_m/B varying with the molar gas composition w in the w domain $[0, 1]$ for each binary gas mixture. Values of the maximum allied convective coefficients $h_{m,max}/B$ attained at the correlative optimal molar gas compositions w_{opt} are easily extracted from a graphical display.

Nomenclature

B	=	related to the mean heat transfer coefficient, Eq. (1)
H	=	side of square cavity, m
h	=	mean heat transfer, $W \cdot m^{-2} \cdot K^{-1}$
M	=	molar mass, $g \cdot mol^{-1}$
R	=	gas constant, $J \cdot mol^{-1} \cdot K^{-1}$
Ra	=	Rayleigh number, $g\beta(T_H - T_C)H^3Pr/\nu^2$
w	=	molar gas composition of a binary gas mixture

Subscripts

a	=	air
m	=	gas mixture
max	=	maximum

I. Introduction

FREE convection flows confined to square cavities occur in several branches of engineering, geophysics, environmental sciences, etc. By solving the steady Navier–Stokes and energy equations, analysts are able to predict laminar convective flows at any Rayleigh number, in principle. Yet as the impressed wall temperature difference rises and/or the sizes of the square cavity grow, all laminar convective flows become turbulent at sufficiently high Rayleigh numbers [1,2]. Many of the laminar convective flows turn oscillatory over a certain range of Rayleigh numbers. The oscillatory regimes usually lie somewhere between the laminar and turbulent regimes [3].

Received 15 August 2005; revision received 6 July 2006; accepted for publication 6 July 2006. Copyright © 2006 by the American Institute of Aeronautics and Astronautics, Inc. All rights reserved. Copies of this paper may be made for personal or internal use, on condition that the copier pay the \$10.00 per-copy fee to the Copyright Clearance Center, Inc., 222 Rosewood Drive, Danvers, MA 01923; include the code \$10.00 in correspondence with the CCC.

*Associate Professor, Department of Mechanical Engineering, 33 Colchester Avenue, 201 Votey Building. Member AIAA.

†Research Associate, Department of Mechanical Engineering, 33 Colchester Avenue, 201 Votey Building.

‡Assistant Professor, College of Science, Department of Chemistry.

A number of numerical and experimental works have been carried out in the past decades in an attempt to predict turbulent convective flows in closed square cavities in a qualitative manner. Representative articles related to numerical predictions are those of Nobile et al. [4], Paolucci [5], and Ampofo and Karayiannis [6]. It is worth noting that the majority of these papers used air while few of them employed water.

The efficacious design of gas-filled square cavities rests on three key elements: 1) the sizing of the cavity, 2) the specification of the temperature difference $T_H - T_C$ at the vertical walls, and 3) the selection of the working fluid. The present study deviates significantly from earlier studies. Instead, the study is centered on special gaseous medium that is expected to perform better than air for purposes of turbulent free convection intensification. Attention is focused primarily on the usage of binary gas mixtures formed with helium (He) and xenon (Xe), although the possibility of mixing other single gases with He is also examined.

II. Physical System

Because the free convection mode comprises the molecular heat conduction mode and fluid motion, one feasible idea for invigorating the free convection mode may revolve around the improvement of the flow characteristics that certain binary gas mixtures offer through their intrinsic thermophysical property values. This indeed is a thermodynamic approach that seeks to exploit the interplay of the four intervening thermophysical properties: viscosity μ , thermal conductivity λ , density ρ , and isobaric heat capacity C_p .

The physical system under study consists of a square cavity of side H with the left wall heated at T_H , the right wall cooled at T_C , and the two connecting horizontal walls insulated from the external air. Five binary gas mixtures are considered in which helium (He) is the primary gas component and carbon dioxide (CO₂), methane (CH₄), nitrogen (N₂), oxygen (O₂), and xenon (Xe) are the secondary gas components.

III. Numerical Model

The numerical calculation procedure is implemented for the analysis of turbulent free convection at $Ra = 2 \times 10^9$, which consists of three sequential steps. First, a molar gas composition w of

Table 1 Molar mass M and molar mass difference ΔM of the pure gases

Single gas	M , g/mol	ΔM with respect to He
He	4.003	—
CH ₄	16.043	12.04
N ₂	28.014	24.01
O ₂	31.999	28.00
CO ₂	44.010	40.00
Xe	131.29	127.87

a binary gas mixture is chosen in the w interval $[0, 1]$. Second, at the reference temperature $T_{\text{ref}} = (T_H + T_C)/2$, the thermophysical properties, viscosity μ_m , thermal conductivity λ_m , density ρ_m , heat capacity at constant pressure $C_{p,m}$, as well as the Prandtl number Pr_m are evaluated (the subscript m implies mixture of gases) [7]. Third, the system of conservation equations is solved by means of the finite volume procedure in conjunction with the ideal gas equation of state $p = \rho RT$, assuming that the air and the five gas mixtures behave as ideal gases. As noted before, turbulence is modeled with the low-Reynolds number $k-\varepsilon$ model.

Based on a sequence of numerical experiments by successively increasing the grid dimensions, it was found that the mesh constructed with 25,000 quadrilateral elements provided a good compromise between the computational efforts and accuracy. The grid independence was achieved within a band of 1%. Because the turbulent natural convection boundary layer is expected to be extremely thin along the heated wall, a nonuniform grid was deployed in the computational domain with nodes tightly clustered near the wall boundaries.

Local convergence was assessed by monitoring the magnitude of the total heat flux across the active walls by setting its variation to less

than 10^{-5} , whereas global convergence was guaranteed by controlling the residuals of the conservation equations to values less than 10^{-6} . The finite volume code was tested against the recent experimental data of Ampofo and Karayiannis [6] using air and good agreement was found. The maximum difference detected did not exceed 15% and 4% for the vertical velocity and temperature profiles, respectively.

IV. Binary Gas Mixtures that Maximize the Heat Transfer Coefficient

From fluid physics, it is expected that the interaction between the four intervening thermophysical properties $\lambda_m(w)$, $\mu_m(w)$, $\rho_m(w)$, and $C_{p,m}(w)$ of the binary mixtures He-Xe, He-N₂, He-O₂, He-CO₂, and He-CH₄ will be able to modify the turbulent velocity and temperature fields in a square cavity in a favorable way. The rationale behind this expectation is explained in this section.

Table 1 lists the mass M of the six single gases He, N₂, O₂, CO₂, CH₄, and Xe, accompanied by the molar mass difference ΔM between each secondary gas N₂, O₂, CO₂, CH₄, and Xe, and the primary gas He. The items in the table indicate that the largest $\Delta M = 127.87$ g/mol correspond to the He-Xe binary mixture. In contrast, the smallest $\Delta M = 12.04$ g/mol corresponds to the He-CH₄ binary mixture. For the five binary mixtures, the variations of the thermophysical properties λ_m , μ_m , ρ_m , and $C_{p,m}$, with the molar composition w at 300 K are illustrated in Fig. 1. The family of curves $\mu_m(w)$, $\lambda_m(w)$, and $\rho_m(w)$ exhibit a common pattern in Figs. 1a–1c. That is, in each figure the uppermost curves are associated with the He-Xe gas mixture having the largest ΔM , as opposed to the lowermost curves which are connected to the He-CH₄ gas mixture having the smallest ΔM . This order is reversed for the family of curves for $C_{p,m}(w)$, namely, the uppermost curve is linked

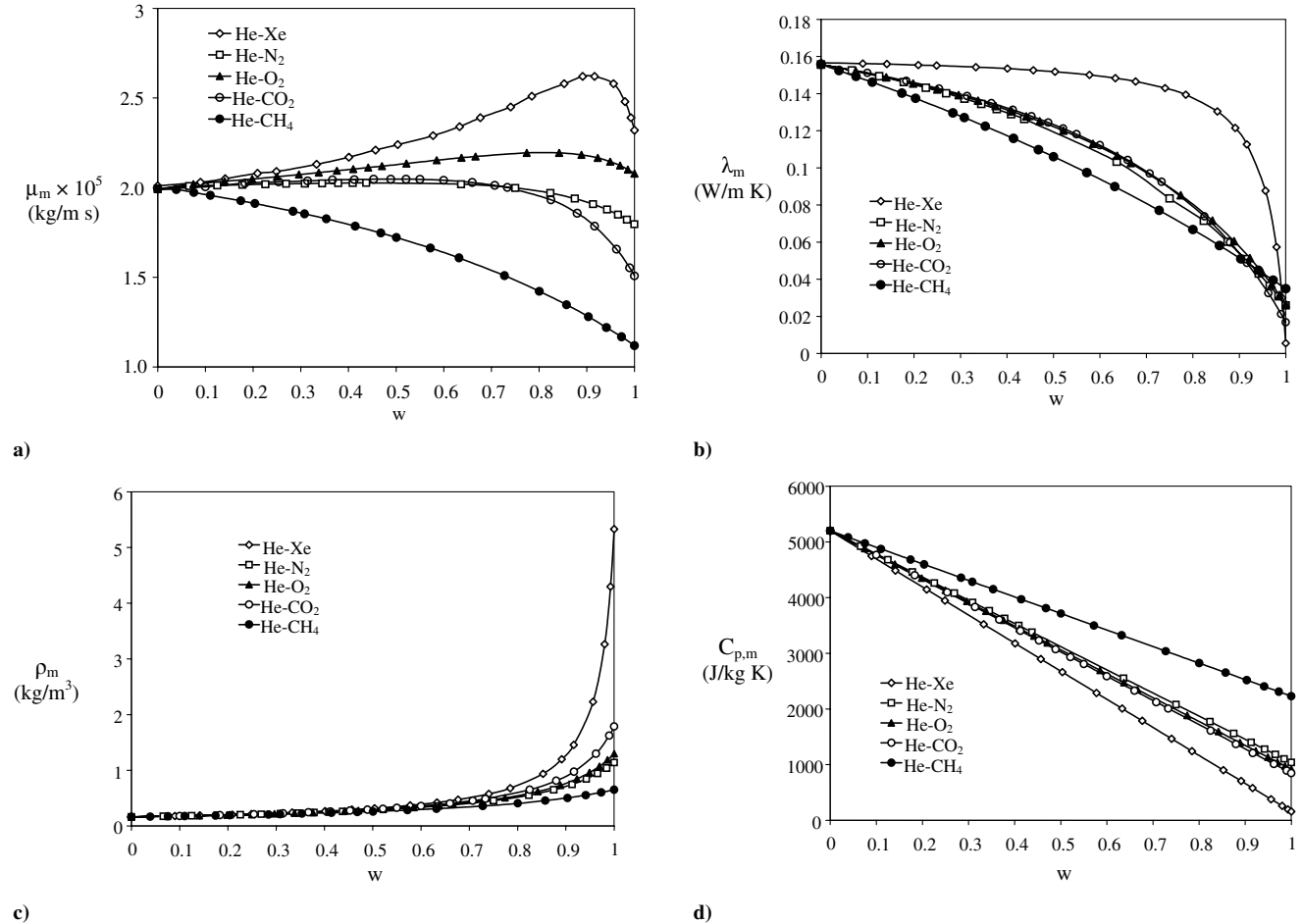


Fig. 1 Evolution of a) the molecular viscosity; b) the thermal conductivity; c) the density; and d) the heat capacity at constant pressure with the molar gas composition of the five binary gas mixtures at $T_{\text{ref}} = 300$ K.

to the He-CH₄ gas mixture, whereas the lowermost curve is linked to the He-Xe gas mixture.

Moreover, a striking peculiarity of the trio of thermophysical properties λ_m , ρ_m , and $C_{p,m}$ is their monotonic changing paths with increments in w . However, the $\mu_m(w)$ curve deviates from this pattern in the sense that the uppermost curve for the He-Xe gas mixture passes through a maximum near $w = 0.9$. Moving down through the other curves, it is observable that the maxima get debilitated. In fact, the lowermost curve for the He-CH₄ gas mixture resembles a negative-sloped straight line.

The aim of this section is to search for the maximum allied heat transfer coefficient h_m/B for the five binary gas mixtures at a preselected film temperature of 300 K that may fall at the optimal molar gas composition w_{opt} . Conceptually, a point $w = w_{\text{opt}}$ is a maximum of the function $h_m/B = f(w)$ if $f(w_{\text{opt}}) > f(w)$ for all w in the proper w domain $[0, 1]$. Hence, the location of w_{opt} furnishes

the optimal molar gas composition of the binary gas mixture that renders a maximum $h_{m,\text{max}}/B$ within all possible ranges that the allied heat transfer coefficients h_m/B can have in the w domain $[0, 1]$.

V. Discussion of Results

The results presented in this section are for $Ra = 2 \times 10^9$ and $T_{\text{ref}} = 300$ K. The structure of the solution channeled through streamlines and isotherms for air and three of the five binary gas mixtures at a molar gas composition $w = 0.93$ (7% He and 93% of a secondary gas component) is given in Fig. 2. From Fig. 2a, we observed a contour plot of the stream function where three counter-rotating vortices coexist; the main vortex of high strength and large size is rotating clockwise and two secondary vortices of small size are located in the upper left and lower right corners of the enclosure. As evidenced from the stream function gradient, the velocity is highest

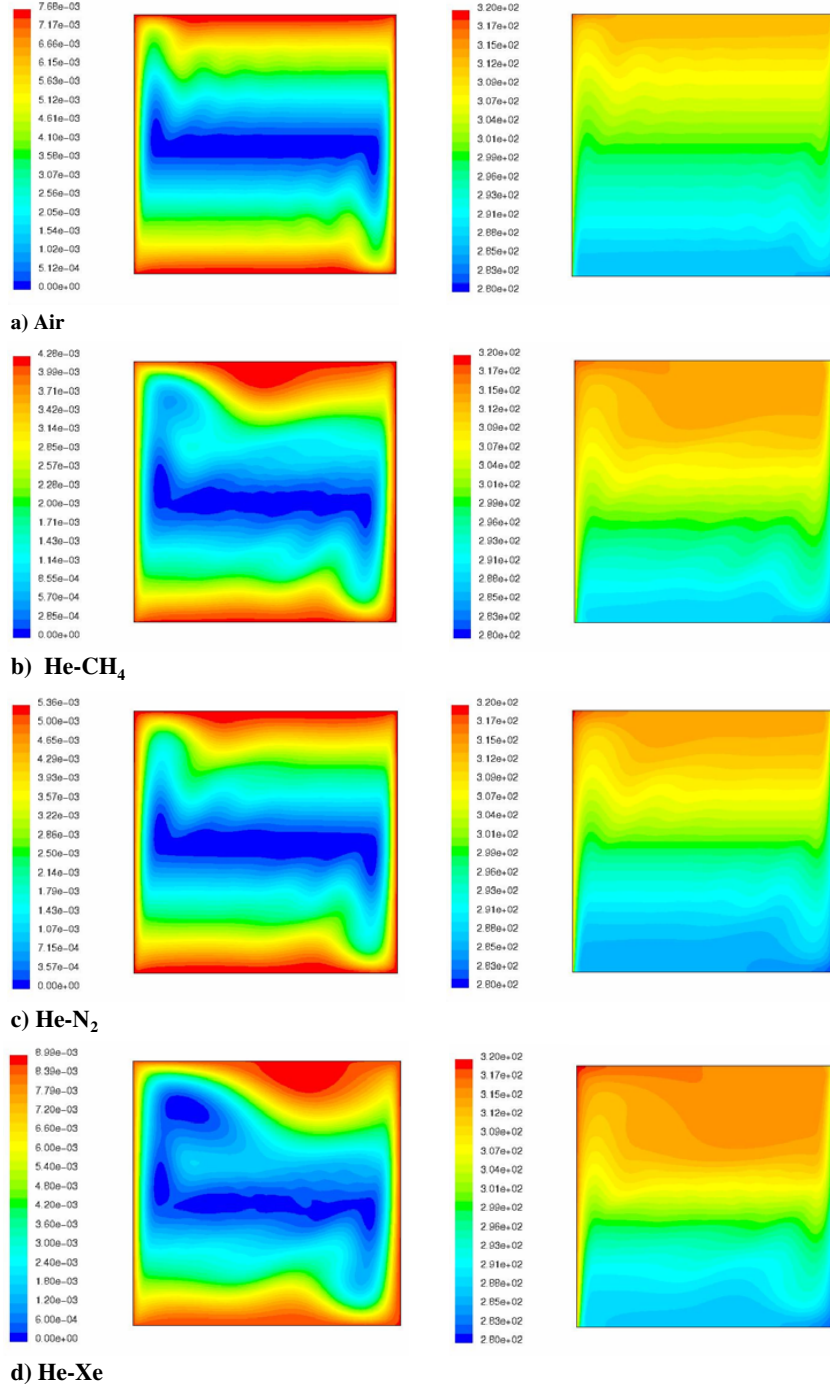


Fig. 2 Velocity and temperature fields at $Ra = 2 \times 10^9$ for a) air; b) He-CH₄ mixture; c) He-N₂ mixture; and d) He-Xe mixture: streamlines on the left and isotherms on the right.

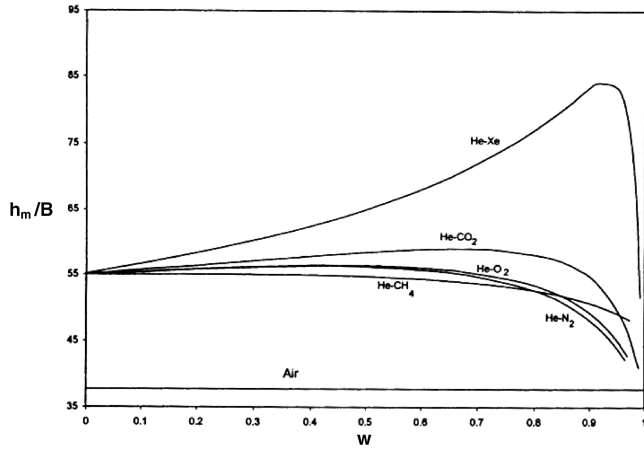


Fig. 3 Variation of the relative mean convective coefficient h_m/B with the molar gas composition of the binary gas mixtures at $T_{\text{ref}} = 300 \text{ K}$ and $Ra = 2 \times 10^9$.

near the vertical active walls and thin boundary layers are formed in these regions. In contrast, the cavity nucleus contains slow moving fluid as shown by the low gradient area in the center. The isotherms indicate a large isothermal core with sharp gradients near the walls. When the He-CH₄ mixture is inserted into the cavity (Fig. 2b), the fluid velocity is reduced significantly compared to the air velocity in Fig. 2a; He-CH₄ is found to display lower velocities also when compared to the other gas mixtures. However, the size of the upper secondary vortex increased resulting in a large isothermal subregion under the upper insulated wall as reflected in the corresponding isothermal plots. The He-N₂ gas mixture in Fig. 2c exhibits flow characteristics that are similar to the ones for air. The fluid velocity and the size of the upper vortex increase when the cavity is filled with He-N₂, He-O₂, and He-CO₂ mixtures, respectively. The He-Xe mixture in Fig. 2d attests the thinnest turbulent boundary layer along the vertical active walls resulting in higher fluid velocities. The upper secondary vortex intensifies and pushes the main vortex down toward the core of the cavity.

In this section we examine how the turbulent boundary layer behaves near the hot wall and how each binary gas mixture is capable of carrying heat away from the wall. The convective heat transfer coefficient at the hot wall can be determined using the calculated temperatures inside the thermal boundary layer.

From a practical perspective, it is convenient to contrast the turbulent free convection performances of the He-Xe gas mixture against that of air, when both gases are confined to square cavities of identical dimensions and are operating at the same temperature. This is done graphically with a figure having the allied convection coefficient h_m/B on the ordinate and the molar gas composition w on the abscissa. In Fig. 3, the format of the abscissa indicates that the left extreme $w = 0$ belongs to the primary gas component He, whereas the right extreme $w = 1$ corresponds to the secondary gas component Xe. Also, the figure contains a horizontal line related to the allied mean convection coefficient for air h_a/B , the so-called baseline case. The constant B was introduced to absorb the gravity acceleration and the temperature difference. For the case of a standard gravity with $g = 9.8 \text{ m/s}^2$, B simplifies to a standardized power law expression

$$B = 0.1 \left(\frac{T_H - T_C}{T_{\text{ref}}} \right)^{1/3} \quad (1)$$

For comparison purposes, at fixed reference temperature $T_{\text{ref}} = 300 \text{ K}$, we used the allied mean convection coefficients for He, $h_{\text{He}}/B = 55$ and for air, $h_a/B = 37.5$. Correspondingly, the heat transfer augmentation $(h_{\text{He}} - h_a)/h_a$ rendered by He with respect to air amounts to a significant 47%.

It is observable in Fig. 3 that the peak of the h_m/B curve for the He-Xe gas mixture is shifted to the upper right part of the plane and an enormous maximum for the allied mean convection coefficient $h_{m,\text{max}}/B = 85$ is furnished in the w domain $[0, 1]$. This particular

ordinate occurs at an optimal molar gas composition $w_{\text{opt}} = 0.93$ (7% He and 93% Xe). Relative to air, the heat transfer maximization $(h_{m,\text{max}} - h_a)/h_a$ delivered by the He-Xe gas mixture ascends to a remarkable 127%. When compared to pure He gas, and again using $(h_{m,\text{max}} - h_a)/h_{\text{He}}$, the He-Xe gas mixture outperforms He by a margin of 55%.

For the He-CO₂ gas mixture, the maximum allied mean convection coefficient $h_{m,\text{max}}/B = 59$ takes place at an optimal molar gas composition $w_{\text{opt}} = 0.7$ (30% He and 70% CO₂). Relative to air, the heat transfer maximization $(h_{m,\text{max}} - h_a)/h_a$ delivered by the He-CO₂ gas mixture is of the order of 57%. When compared to He and employing $(h_{m,\text{max}} - h_a)/h_{\text{He}}$, the He-CO₂ gas mixture outperforms He by a slight margin of 7%. The He-O₂ and He-N₂ gas mixtures furnish imperceptible maxima for the allied mean convection coefficient h_m/B that have minimal significance. Lastly, it is obvious that the allied mean convection coefficient h_m/B for the He-CH₄ gas mixture does not pass through a maximum.

The trends observed in Fig. 3 and Table 1 suggest that the allied convection coefficients $h_{m,\text{max}}/B$ respond to the molar mass difference ΔM between the primary gas He and the secondary gas Xe. As noted in Table 1, the He-Xe gas mixture possesses the largest molar mass difference $\Delta M = 127.87 \text{ g/mol}$, which translates into the global maximum allied mean convection coefficient $h_m/B = 85$. The He-CO₂ gas mixture with the second largest molar mass difference $\Delta M = 40 \text{ g/mol}$ comes in a distant second. The smallest $\Delta M = 12.04 \text{ g/mol}$ for the He-CH₄ gas mixture reveals no maximum allied mean convection coefficient h_m/B .

VI. Conclusions

A numerical investigation of two-dimensional turbulent free convection in square cavities filled with a binary gas mixture was conducted for a fixed Rayleigh number, $Ra = 2 \times 10^9$ at the reference temperature, $T_{\text{ref}} = 300 \text{ K}$. The gas flows in a narrow strip along the walls where the velocity and temperature change sharply. The He-Xe mixture delivers the thinnest turbulent boundary layers along the vertical active walls resulting in higher fluid velocities. The He-Xe is the best gas mixture choice for heat transfer enhancement within square cavities. The latter transfers 127% more heat than air. When compared to pure He, the heat transfer gain of about 55% is obtained. The maximum heat transfer coefficient occurs at an optimal molar gas composition $w_{\text{opt}} = 0.93$. For the He-CO₂ gas mixture, the maximum takes place at an optimal molar gas composition $w_{\text{opt}} = 0.7$. Relative to air, the heat transfer maximization delivered by the He-CO₂ gas mixture is of the order of 57%. Other gas mixtures present limited heat transfer enhancements.

References

- [1] Raithby, G. D., and Hollands, K. G. T., "Natural Convection," *Handbook of Heat Transfer*, 3rd ed., edited by W. M. Rohsenow, J. P. Hartnett, and Y. I. Cho, McGraw-Hill, New York, 1998, Chap. 4.
- [2] Jaluria, Y., "Natural Convection," *Heat Transfer Handbook*, edited by A. Bejan and A. D. Kraus, Wiley, New York, 2003, Chap. 7.
- [3] LeQuéré, P., and Alziari de Roquefort, T., "Transition to Unsteady Natural Convection of Air in Vertical Differentially Heated Cavities: Influence of Thermal Boundary Conditions on the Horizontal Walls," *Proceedings of the 8th International Heat Transfer Conference*, Hemisphere Publishing Corp., Washington, D.C., 1986.
- [4] Nobile, E., Sousa, A. C. M., and Barozzi, G. S., "Turbulent Modelling in Confined Natural Convection," *International Journal of Heat Technology*, Vol. 7, No. 1, 1989, pp. 24–35.
- [5] Paolucci, S., "Direct Numerical Simulation of Two-Dimensional Turbulent Natural Convection in an Enclosed Cavity," *Journal of Fluid Mechanics*, Vol. 215, June 1990, pp. 229–262.
- [6] Ampofo, F., and Karayiannis, T. G., "Experimental Benchmark Data for Turbulent Natural Convection in an Air Filled Square Cavity," *International Journal of Heat and Mass Transfer*, Vol. 46, No. 19, 2003, pp. 3551–3572.
- [7] Poling, B. E., Prausnitz, J. M., and O'Connell, J. P., "The Properties of Gases and Liquids," McGraw-Hill, New York, 2001, A.5–A.19.